Supporting Information

Condello et al. 10.1073/pnas.1714966115

SI Methods

Transgenic Mice. Tg(APP23) mice expressing Swedish mutant human APP (751-amino acid isoform) under the control of the *Thy-1.2* promoter (1) were a gift from Matthias Staufenbiel, Department of Cellular Neurology, Hertie Institute for Clinical Brain Research, University of Tübingen, Tübingen, Germany, and were maintained on a C57BL/6-Stein background. Tg(*Gfap*-luc) mice expressing firefly luciferase under the control of the murine *Gfap* promoter (2) were a gift from Caliper Life Sciences, Hopkinton, MA, and were maintained on an FVB/N background. Homozygous Tg(*Gfap*-luc) mice were generated by intercrossing hemizygous animals and were confirmed by backcrossing. To create bigenic mice, Tg(APP23) mice were crossed with homozygous Tg(*Gfap*-luc) animals. Equal numbers of male and female mice were used for all experiments. Animals were maintained in a facility accredited by the Association for Assessment and Accreditation of Laboratory Animal Care International in accordance with the *Guide for the Care and Use of Laboratory Animals* (3). All procedures for animal use were approved by the University of California, San Francisco's Institutional Animal Care and Use Committee.

Mouse Inoculations. Synthetic Aβ fibril samples were adjusted to 0.4 mg/mL in PBS, and 30 μL of synthetic Aβ aggregates were inoculated into 2-mo-old Tg(APP23:*Gfap*-luc) mice into the right cerebral hemisphere (thalamus) using a 27-gauge syringe, a method commonly employed to deliver PrP prions. Mice were killed at 330 d postinoculation for biochemical and histological analysis.

Quantification of Amyloid Plaque Immune-Labeled Aβ Isoform Fluorescence. Aβ38 and Aβ40 fluorescence intensities of individual amyloid plaques were imaged with a 40× water immersion lens (1.1 NA) in sequential scan mode and analyzed with NIH ImageJ software. A *z*-projection of four confocal optical slices through the center of the plaque core was prepared from each image *z*-stack and used for analysis. A standard region of interest was used to measure the intensities of Aβ38 and Aβ40 fluorescence along the plaque core perimeter as demarcated by FSB labeling. Multiple regions of interest were acquired per individual plaque and were used to calculate the average ratio of Aβ38/Aβ40 fluorescence. Brain slices from three to five animals per experimental or control group were used for quantification.

Statistical Methods Used for Data Analysis. Statistical analysis of Aβ38 and Aβ40 levels were performed using Prism 6 software (GraphPad Software). Statistical differences between groups were assessed using unpaired, two-tailed *t* tests or by performing one-way ANOVA with Tukey's multiple comparison posttest. A significance threshold of $P = 0.05$ was used for all experiments.

Preparation of Synthetic Aβ Aggregates. WT Aβ40 and Aβ38 and E22Q Aβ40 peptides were purchased from Bachem. The Arctic mutant peptide (1–38 and 1–40) was synthesized using a Biotage Initiator+ Alstra automated microwave peptide synthesizer on Val-HMPB-Chemmatrix resin (loading 0.5 mmol/g, 0.1 mmol scale). Fmoc deprotection was performed at 70 °C using 0.1 M HOBt in 4-methyl piperidine-DMF (1:4) for 5 min. The resin was then washed with DMF (3×). Coupling reactions were performed using Nα-Fmoc amino acids (5 equivalent, 0.5 M), HCTU (4.95 equivalent, 0.5 M), and DIEA (10 equivalent, 0.5 M) in DMF. All couplings were doubly performed for 5 min at 75 °C except for His (25-min double coupling at room temperature) and Arg (5-min triple coupling at 75 °C). After completion of synthesis, the resin was successively washed with DMF (3×) and DCM (3×) and dried. Peptide cleavage was performed using TFA-DTT-H_2O (95:2.5:2.5) for 3 h at room temperature. The volatiles were removed by a stream of nitrogen, and the crude peptide was obtained by precipitation with cold diethyl ether. The crude peptide was dissolved in hexafluoro-isopropanol (HFIP) and purified by RP-HPLC. A portion of the crude solution was injected into the heated (60 °C) Vydac 300 Å C4 column (214TP1022, 10 μM, 22 × 250 mm), running a flow of 10 mL/min with a linear gradient from 15 to 40% of buffer B over 25 min [buffer A: 0.1% TFA in H_2O; buffer B: 0.1% TFA in CH_3CN-H_2O (99:1)]. Mass analysis was performed using electrospray ionization-MS (Qtrap 3200; ABSCI EX). The Aβ (1–38) peptide (H-DAEFRHDSGYEV-HHQKLVFFAE-DVGSNKGAII-GLMVGG-OH) was similarly prepared on Gly-HMPB-Chemmatrix resin.

Lyophilized peptides were dissolved to 5 mg/mL in HFIP and separated in 200-μg aliquots. HFIP was evaporated in a speedvac and stored at −20 °C. For conversion, the dried peptide film was solubilized in 20 μL DMSO and diluted with 980 μL of aqueous buffer solutions containing 10 mM NaP. Samples were incubated at 37 °C for 72 h in 1.5-mL centrifugation tubes under constant agitation at 900 rpm in a DELFIA Plateshake instrument (PerkinElmer). For bioassays in Tg(APP23) mice, resulting amyloids were spun down for 1 h at 100,000 × *g*, and the pellet was resuspended in 500 μL PBS at 0.4 mg/mL. Samples were further analyzed or snap-frozen and stored at −80 °C before inoculation.

Proteinase K Digestion of Synthetic Aβ Aggregates. After incubation for 72 h at 37 °C, synthetic Aβ samples in PBS were adjusted to 200 μg/mL with PBS, and proteinase K (PK) (Thermo Scientific) was added to a final concentration of 50 μg/mL. After digestion for 1 h at 37 °C under constant agitation, the reaction was stopped by the addition of 1 mM PMSF. NuPAGE sample buffer (4×, Invitrogen) was added to a final concentration of 1× before SDS/PAGE.

Kinetic Measurements Using ThT. For spontaneous or seeded kinetic measurements, 100-μL aliquots of synthetic Aβ were adjusted to a final ThT concentration of 10 μM and added to 96-well Lo-Bind plates (Corning). Plates were sealed with a clear film (Nunc) and then incubated in a Spectramax M5 plate reader (Molecular Devices) at 37 °C. Samples were subjected to repeated rounds of 1-min rest and 4-min shaking, and top-read fluorescence measurements (444-nm excitation and 485-nm emission filters) were taken every 5 min over the course of aggregation.

Solution NMR of Aβ Peptides. All spectra were recorded at 249.5 K on a Bruker Avance II 900 MHz spectrometer equipped with a cryogenic probe. During the 1-wk experiment time, all samples were kept in the sample changer with a constant temperature of 249.5 K. One-dimensional spectra were recorded with the Bruker pulse sequence zgesgp with t_{max} = 150 ms, 256 scans. The ^1H carrier frequency was set at 4.60 ppm. All spectra were processed and analyzed using the program TopSpin (Bruker).

SDS/PAGE, Immunoblotting, and Silver Staining. SDS/PAGE was performed using 4–12% Bis-Tris gradient gels (Invitrogen) according to the manufacturer's protocol. Silver staining was carried out according to the protocol of Merril et al. (4).

Immobilization of Synthetic Aβ Fibrils in Agarose Gel. Preformed synthetic Aβ fibrils were mixed with a solution of 0.5% low-melting point agarose (Sigma A9414) in double-distilled water.

The fibril-agarose mixture was then pipetted into a "half area" 96-well microplate (Grenier Bio-One 675096) at 2 μg fibrils per well. Following gel formation, samples are washed with distilled water on a shaker to remove any debris. Fluorescent amyloid dyes were dissolved in distilled water (50 μM ThT, 20 μM curcumin, 10 μM FSB, and 10 μM BF-188) and applied to each well to incubate with immobilized fibrils for 30-min shaking at room temperature. After staining, dye solutions were removed and wells were washed twice with water shaking. A final volume of water was added to keep the gels hydrated for storage and imaging.

1. Sturchler-Pierrat C, et al. (1997) Two amyloid precursor protein transgenic mouse models with Alzheimer disease-like pathology. *Proc Natl Acad Sci USA* 94:13287–13292.
2. Zhu L, et al. (2004) Non-invasive imaging of GFAP expression after neuronal damage in mice. *Neurosci Lett* 367:210–212.
3. Committee for the Update of the Guide for the Care and Use of Laboratory Animals IfLAR; Division of Earth and Life Sciences; National Research Council of the National Academies (2011) *Guide for the Care and Use of Laboratory Animals* (The National Academies Press, Washington, DC), 8th Ed.
4. Merril CR, Dunau ML, Goldman D (1981) A rapid sensitive silver stain for polypeptides in polyacrylamide gels. *Anal Biochem* 110:201–207.

A

	sAD		fAD(E22G)		fCAA(E22Q)	
	Parenchymal	Vascular	Parenchymal	Vascular	Parenchymal	Vascular
BF-188	75.7 ±45.9	81.1 ±48.3	9.3 ± 8.3 (p<0.0001)	8.9 ± 4.9 (p<0.0001)	NA	22.0 ± 8.9 (p<0.0001)
FSB	86.9 ± 45.4	118.3±29.1	12.9 ± 14.9 (p<0.0001)	19.3 ± 7.4 (p<0.0001)	NA	45.7 ± 25.6 (p<0.0001)
Curcumin	64.7 ±34.3	109.1 ±26.3	35.5 ±18.3 (p<0.0001)	63.7 ± 25.1 (p<0.0001)	NA	64.9 ± 26.2 (p<0.0001)
BTA-1	79.3 ±31.6	79.5 ±38.5	2.2 ±4.9 (p<0.0001)	17 ± 8.4 (p<0.0001)	NA	21.1 ± 18.2 (p<0.0001)

B

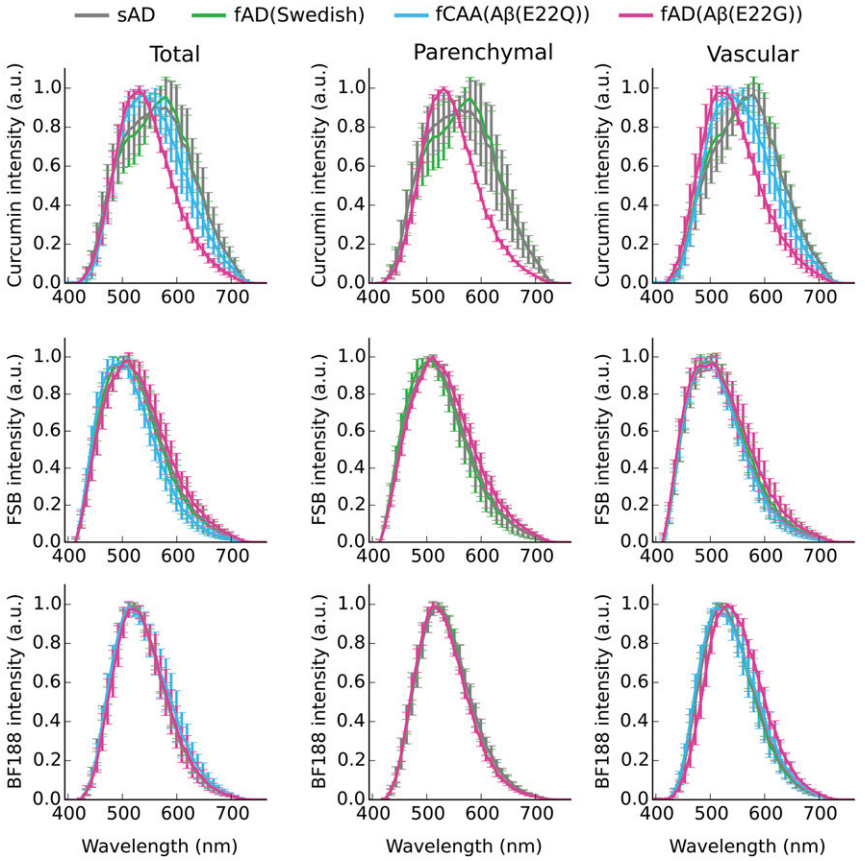

Fig. S1. Fluorescence intensity and confocal spectral imaging of different amyloid-binding probes in sAD and fAD human brain samples. (*A*) Full summary of mean fluorescence intensities of amyloid probes (BF-188, FSB, curcumin, and BTA-1) measured by confocal imaging in sAD and fAD samples. Aβ deposits were measured in the gray matter of the brain ("parenchymal") and along the walls of the cerebrovasculature ("vascular"), also known as CAA. Data shown as mean ± SD. (*B*) Confocal microscopy-based emission spectra from curcumin-, FSB-, and BF-188–labeled Aβ of parenchymal and vascular deposits. Sampling for curcumin: $n = 971$ parenchymal/272 vascular deposits from 21 sAD cases; 243 parenchymal/137 vascular deposits from six fAD (Swedish) cases; 332 parenchymal/134 vascular deposits from five fAD [Aβ(E22G)] (Arctic) cases; 319 vascular deposits from eight fCAA [Aβ(E22Q)] (Dutch) cases. Sampling for FSB: $n = 1{,}069$ parenchymal/202 vascular deposits from 21 sAD cases; 306 parenchymal/137 vascular deposits from six fAD (Swedish) cases; 215 parenchymal/113 vascular deposits from five fAD [Aβ(E22G)] cases; 255 vascular deposits from eight fCAA [Aβ(E22Q)] cases. Sampling for BF-188: $n = 1{,}224$ parenchymal/186 vascular deposits from 21 sAD cases; 334 parenchymal/138 vascular deposits from six fAD (Swedish) cases; 227 parenchymal/102 vascular deposits from five fAD [Aβ(E22G)] cases; 229 vascular deposits from eight fCAA [Aβ(E22Q)] cases. Data shown as mean ± SD.

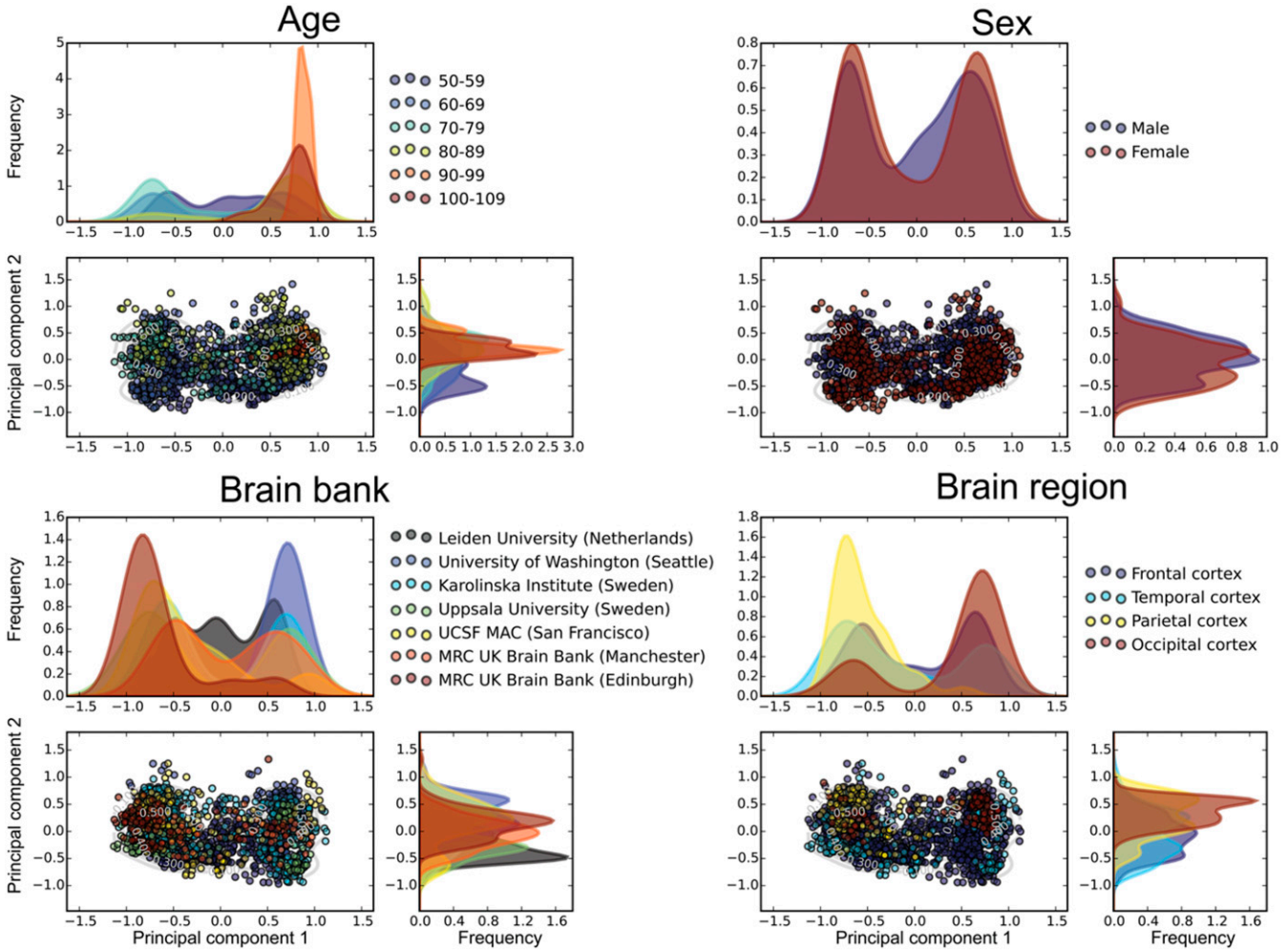

Fig. S2. Intersubject variability of amyloid deposits found in sAD, fAD (Swedish), fAD [Aβ(E22G)], and fCAA [Aβ(E22Q)] samples assessed by patient clinical and demographic details. PCA of spectral data from all disease groups compared by patient age at death, patient sex, source of brain sample (brain bank), and the brain region of each sample.

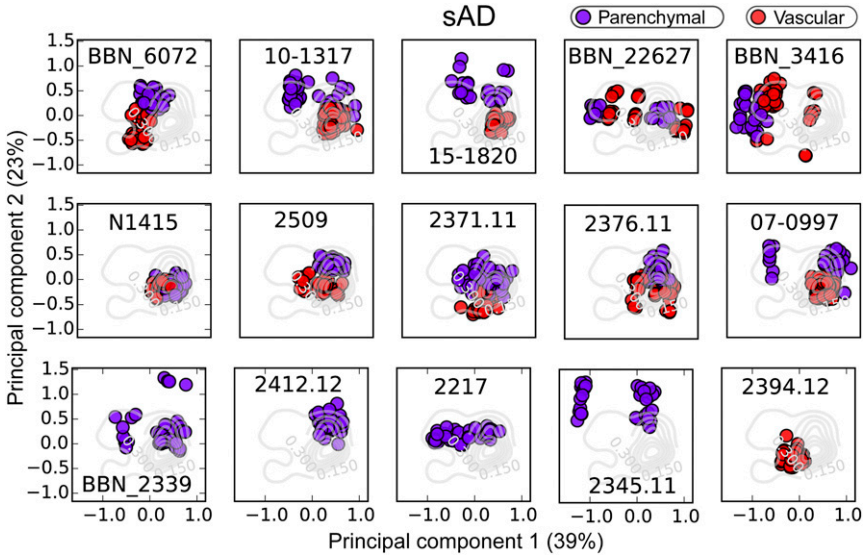

Fig. S3. Effect of the localization of the deposits on the Aβ conformations in sAD patients. These data are an extension of Fig. 4, showing additional 2D fingerprints for all other sAD patients analyzed in this study. The multispectral vectors from sAD patients are projected into the eigenspace defined by the first two components of the PCA. Data are indicated according to the localization of the aggregates in the brain tissue, with parenchymal deposits shown in purple and vascular deposits in red.

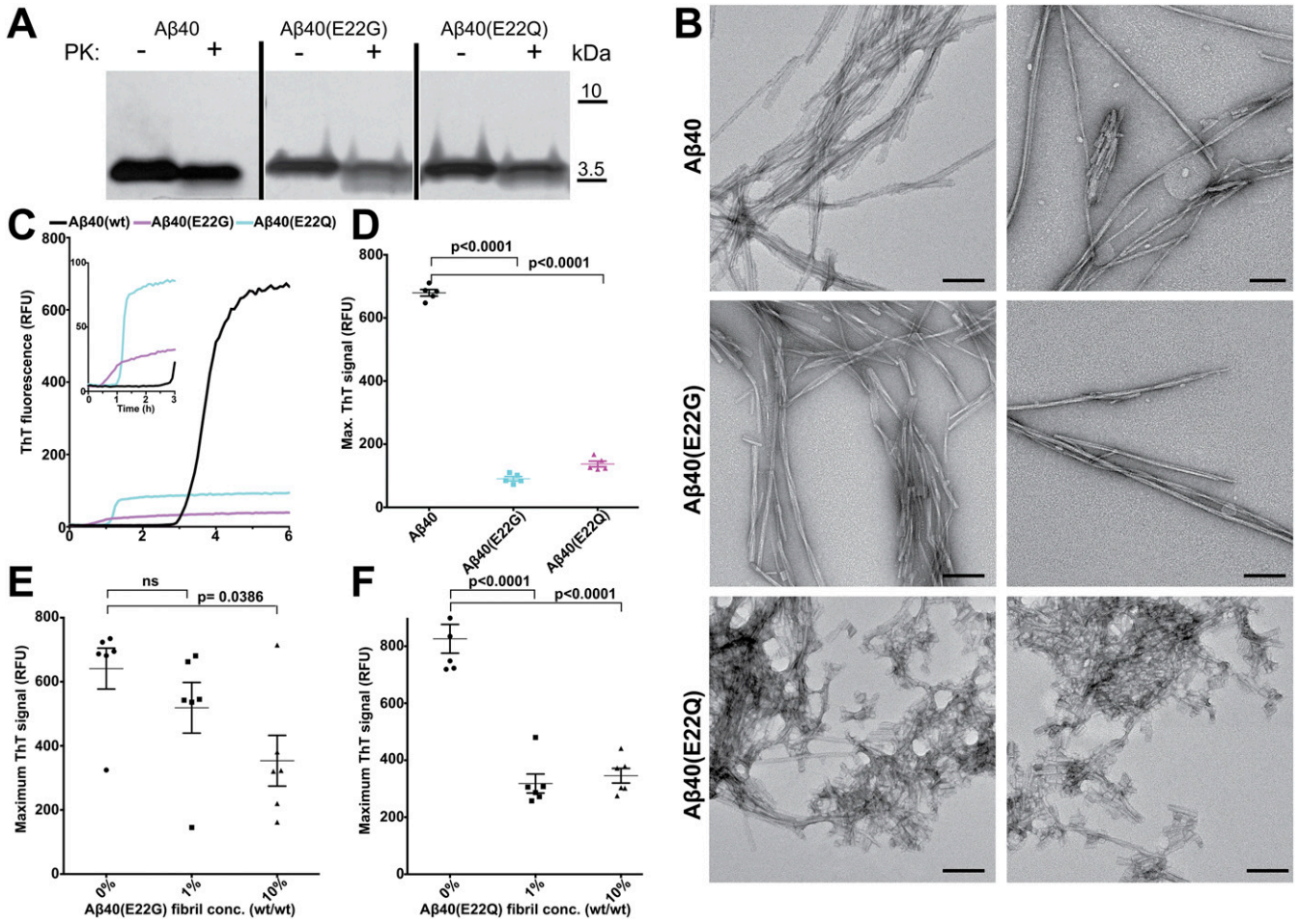

Fig. S4. Characterization of synthetic WT and mutant Aβ40 fibrils. (*A*) Substantial amounts of WT or mutant Aβ (E22G or E22Q) amyloid fibrils showed PK resistance. Following amyloid formation, Aβ fibrils (0.2 mg/mL) were subjected to treatment with 0.05 mg/mL PK for 1 h (37 °C). PK (–) and PK-resistant (+) synthetic Aβ fibrils were visualized by silver staining following SDS/PAGE. (*B*) Representative electron micrographs showing fibrillar ultrastructures of WT Aβ40 and mutant Aβ40(E22G) and Aβ40(E22Q) prions formed under constant agitation for 72 h in phosphate buffer (pH 7.2) at 37 °C. (Scale bars: 100 nm.) (*C*) Kinetics of mutant and WT Aβ40 amyloid formation in vitro (0.2 mg/mL Aβ; 10 μM ThT, 10 mM NaP pH 7.3, 37 °C). (*D*) Endpoint measurements of ThT fluorescence of WT Aβ and mutant Aβ40(E22G) or Aβ40(E22Q) used for seeding in *E* and *F*. Both mutant Aβ40 amyloids show significantly lower ThT fluorescence compared with WT Aβ40 amyloids. (*E* and *F*) WT Aβ40 was templated by either 10% or 1% (wt/wt) preformed mutant Aβ40 fibrils, and six independent replicates are shown for each reaction. Each data point represents the maximum ThT value after an incubation time of 8 h. Aβ40(E22G) and Aβ40(E22Q) were able to convert WT Aβ40 into amyloid structures with similar ThT binding properties compared with the unseeded Aβ40 control. In comparison, Aβ40(E22Q) fibrils were able to template Aβ40 into a different conformation at much lower fibril concentrations than Aβ40(E22G).

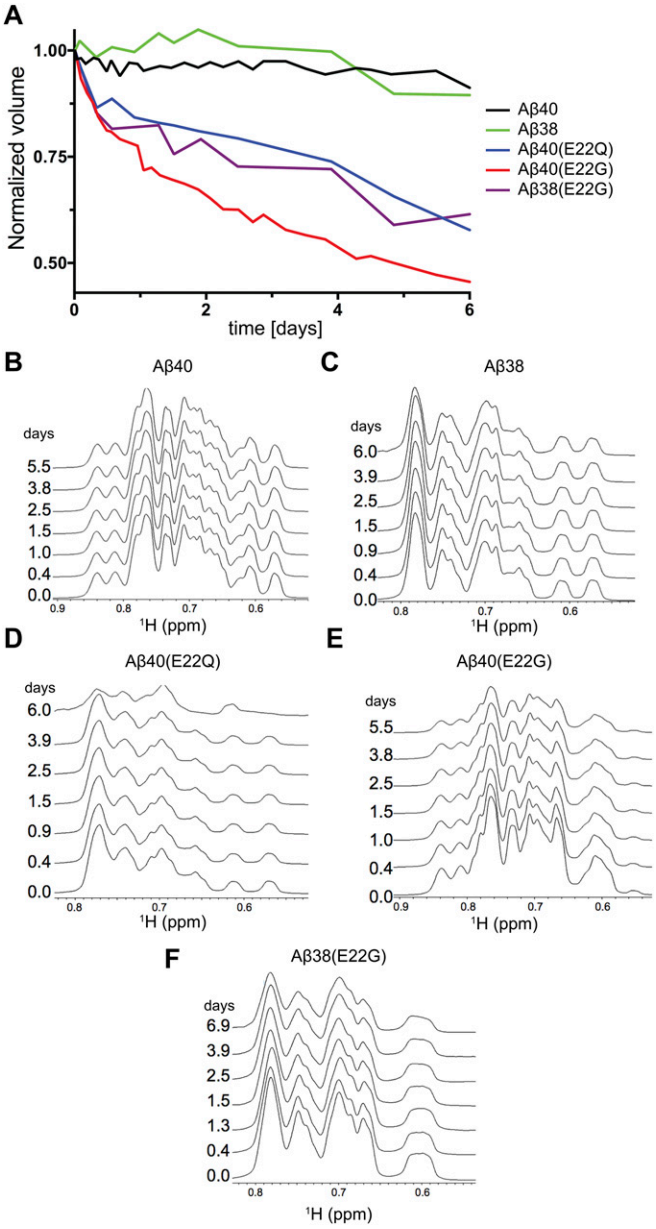

Fig. S5. Label-free monitoring of Aβ multimerization reveals accelerated kinetics for mutant constructs. Solution 1D ^{1}H NMR spectra of WT and mutant Aβ at the methyl group region were monitored over a period of 1 wk. These experiments were designed to test the relative solubility of the different constructs under conditions that are not very conducive to aggregation (i.e., no shaking as in the ThT fibrillization assay). (*A*) All peaks were integrated between 0.5 and 0.9 ppm as a function of time over a period of 6 d. WT Aβ40 and Aβ38 are stable as monomers or small oligomers, whereas Aβ peptides carrying either the E22G or E22Q mutation form large oligomers/aggregates that are undetectable by NMR. (*B*–*F*) Representative 1D ^{1}H NMR spectra were recorded on a 900-MHz NMR spectrometer at 294.5 K. A starting concentration of 100 μm was used for all samples.

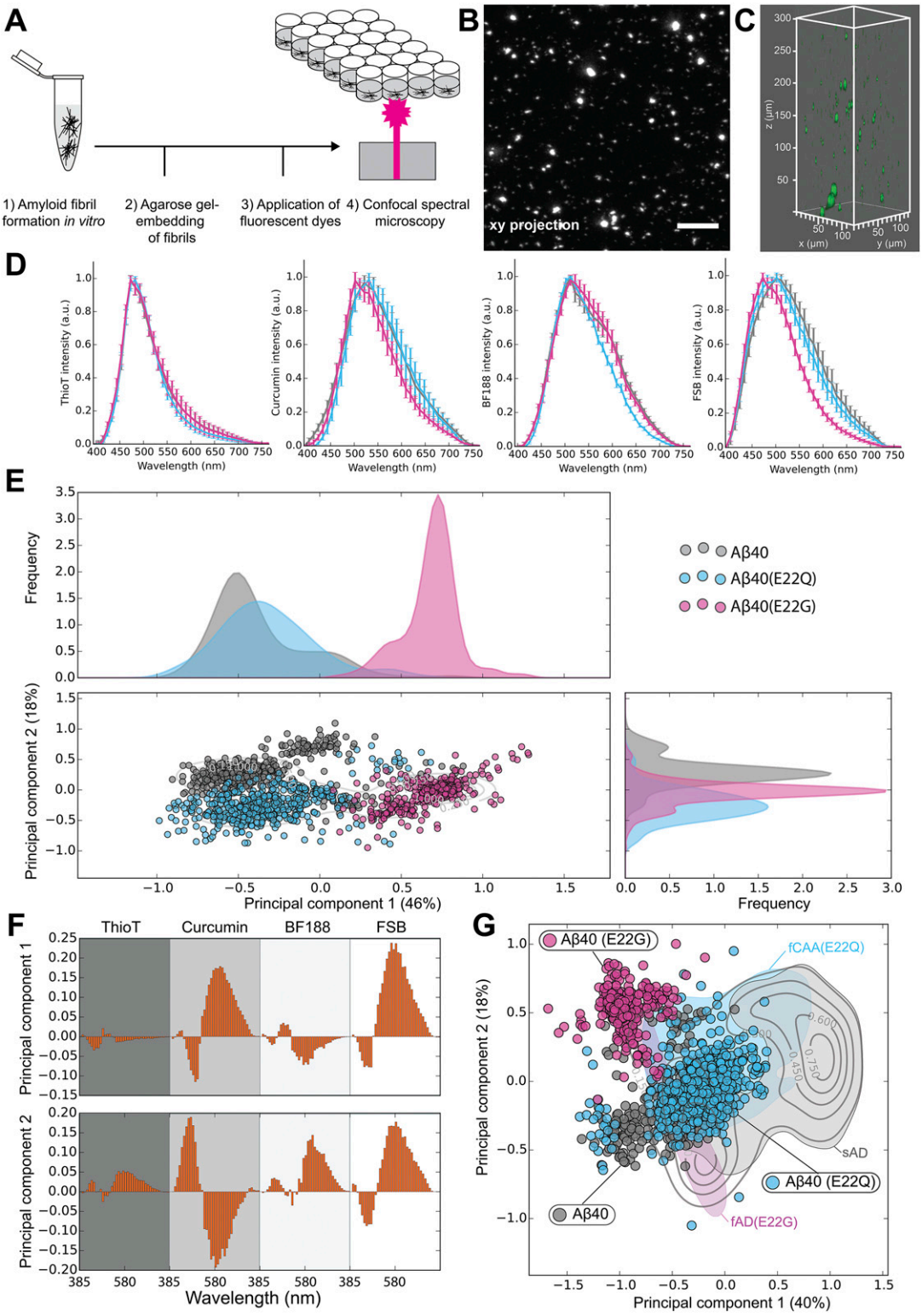

Fig. S6. Gel-embedded synthetic Aβ40 fibrils for 3D confocal spectral imaging. (*A*) Schematic workflow for preparing agarose gel-embedded synthetic Aβ40 aggregates for confocal-based spectral imaging. (*B*) Confocal *xy* projection. (Scale bar, 20 μm.) (*C*) Three-dimensional reconstruction of an entire *z*-stack from a single 63× field of view. (*D*) Confocal-based spectral analysis of ThT, curcumin, BF-188, and FSB fluorescence emission profiles when bound to gel-embedded Aβ40, Aβ40(E22G), and Aβ40(E22Q) fibrils. (ThT analysis: n = 3,126 aggregates. Curcumin analysis: n = 2,944 aggregates. BF-188 analysis: n = 2,385 aggregates. FSB analysis: n = 1,585 aggregates. Data shown as mean ± SD). (*E*) Projection of the multispectral vector into the eigenspace defined by the two first components of the PCA. (*F*) Multispectral vectors from synthetic fibrils are projected into the eigenspace defined in *E*, and their magnitudes reveal the wavelength-dependent contributions from the various dyes to the variation between the samples. (*G*) Projection of the multispectral vector into the eigenspace defined by the human and synthetic samples. The regions occupied by human sAD, fAD(E22Q), and fAD(E22G) are shown in gray, cyan, and magenta, respectively.

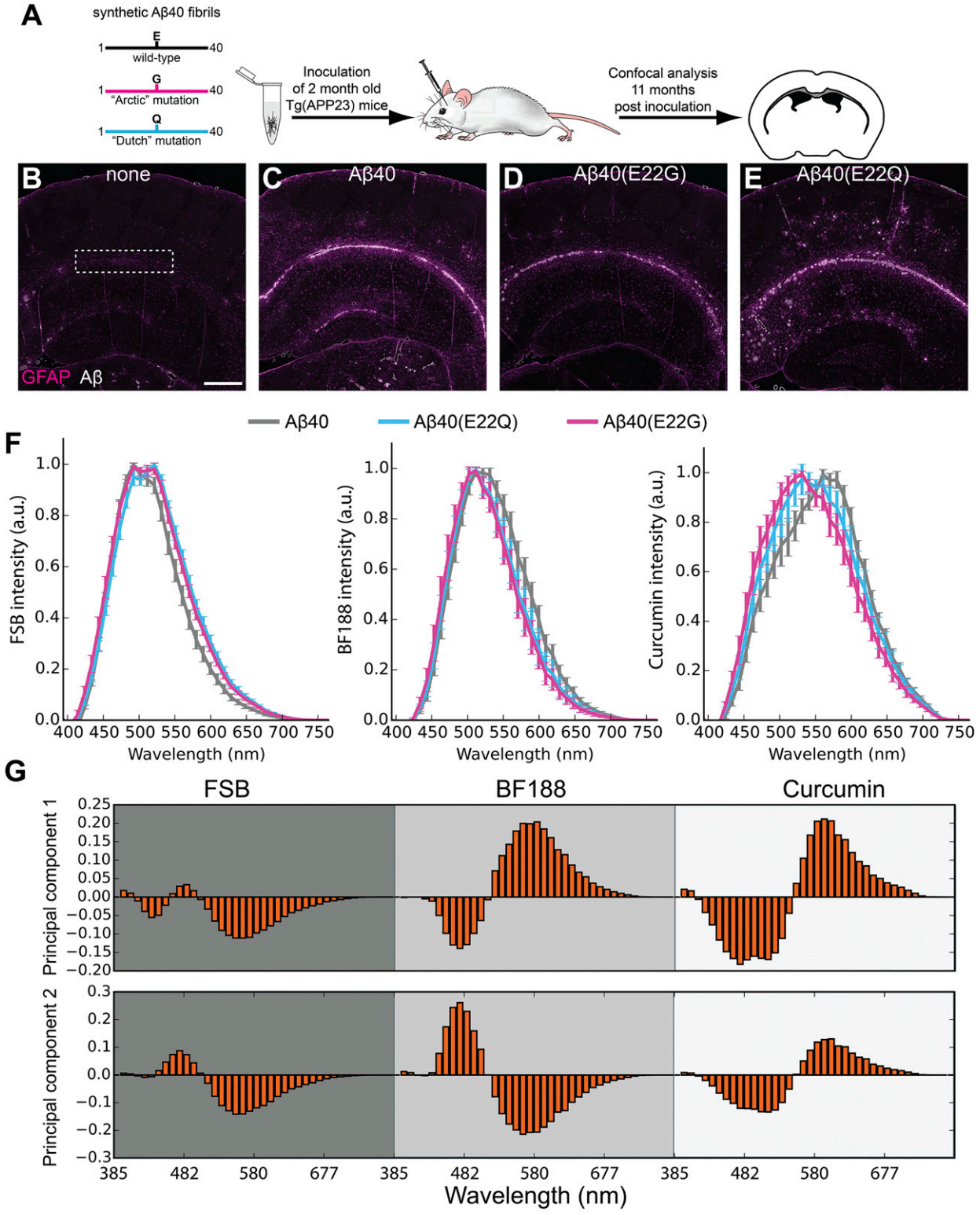

Fig. S7. Transmission of synthetic mutant Aβ40 fibrils to mice expressing WT Aβ. (*A*) Experimental paradigm for transmission of synthetic WT and mutant Aβ fibrils to Tg(APP23) mice. Mice were intracerebrally inoculated at 2 mo of age. Their brains were analyzed after an 11-mo incubation period. (*B–E*) Brain-slice staining for Aβ (Aβ1–16 epitope) and GFAP-immunolabeled astrocytes reveal the stereotypical deposition pattern induced in the corpus callosum above the CA1 region of the hippocampus following thalamic injection. (Scale bar, 500 μm.) (*C*) Aβ40, (*D*) Aβ40(E22G), and (*E*) Aβ40(E22Q) are compared with the uninoculated age-matched control (*B*). (*F*) Confocal-based spectral imaging analysis of FSB, BF-188, or curcumin fluorescence emission profiles from the induced Aβ deposits of the corpus callosum/CA1 hippocampal region is shown. FSB analysis: $n = 4–5$ animals per group/205 plaques. BF-188 analysis: $n = 4–5$ animals per group/896 plaques. Curcumin analysis: Four to five animals per group/720 plaques. Data shown as mean ± SD. (*G*) Multispectral vectors from representative Tg mice are projected into the eigenspace defined in Fig. 5G, and their magnitudes reveal the wavelength-dependent contributions from the various dyes to the variation between the samples.

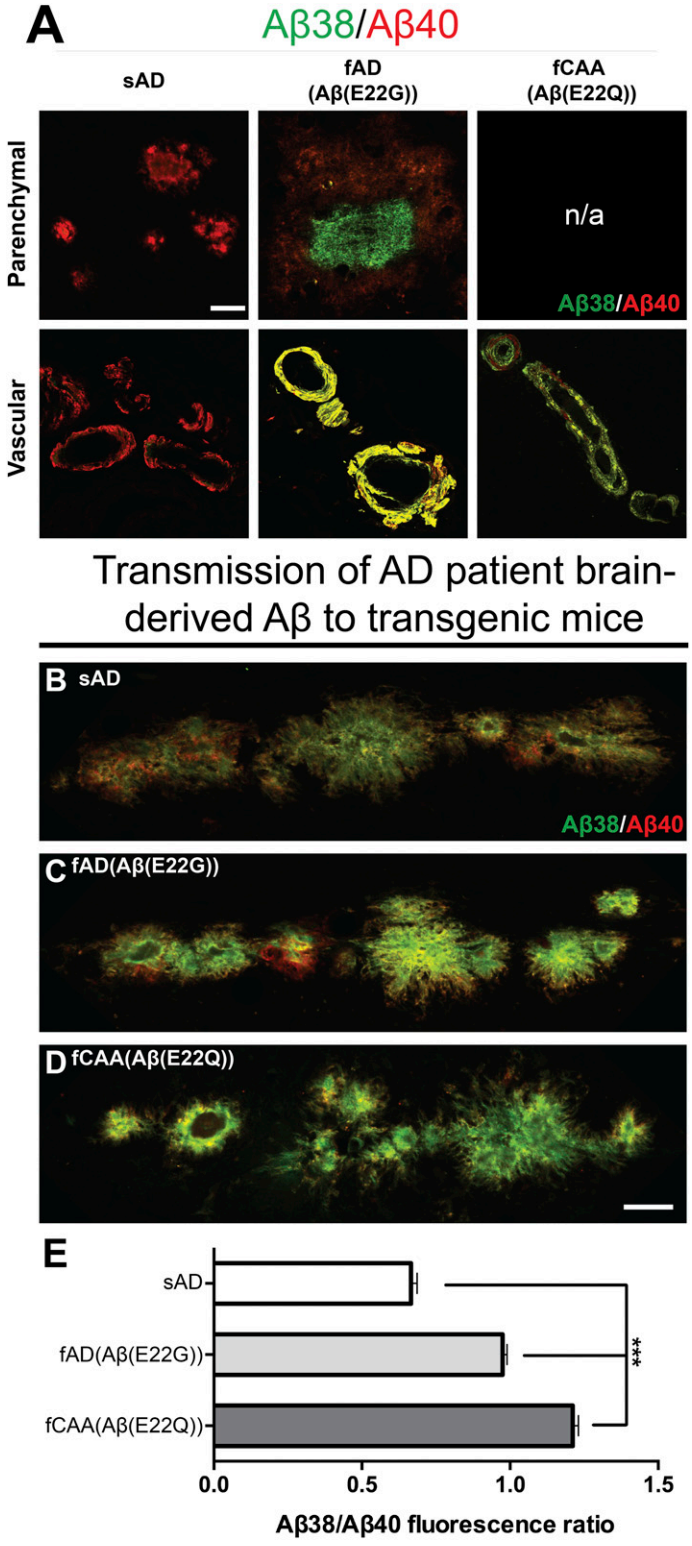

Fig. S8. Transmission of patient-derived fAD brain samples into Tg mice induces Aβ38 incorporation into plaques. (*A*) Confocal images show parenchymal Aβ plaques (*Upper*) and cerebral amyloid angiopathy ("vascular," *Lower*) immunolabeled with C-terminal specific antibodies targeting the Aβ isoform species Aβ38 (green) and Aβ40 (red) in postmortem brain samples from the following cases: (*i*) sAD, (*ii*) fAD [Aβ(E22G)], and (*iii*) fCAA [Aβ(E22Q)]. (*B–E*) Following transmission of mutant Aβ prions derived from patient brain into Tg(APP23) mice induced distinct patterns of Aβ isoform deposition in the corpus callosum/CA1 hippocampal region of Tg mice expressing WT Aβ. (*B–D*) Confocal images show Aβ38 (green) and Aβ40 (red) immunopositive plaques in mice inoculated with (*B*) sAD, (*C*) fAD [Aβ(E22G)], or (*D*) fCAA [Aβ(E22Q)] patient brain homogenate. (*E*) Quantification of Aβ38 and Aβ40 levels (n = 2–3 animals per group/313 plaques). Data shown as mean ± SEM. A one-way ANOVA with Tukey's post hoc statistical test was used. (Scale bars, 25 μm.) ***$P < 0.0001$.

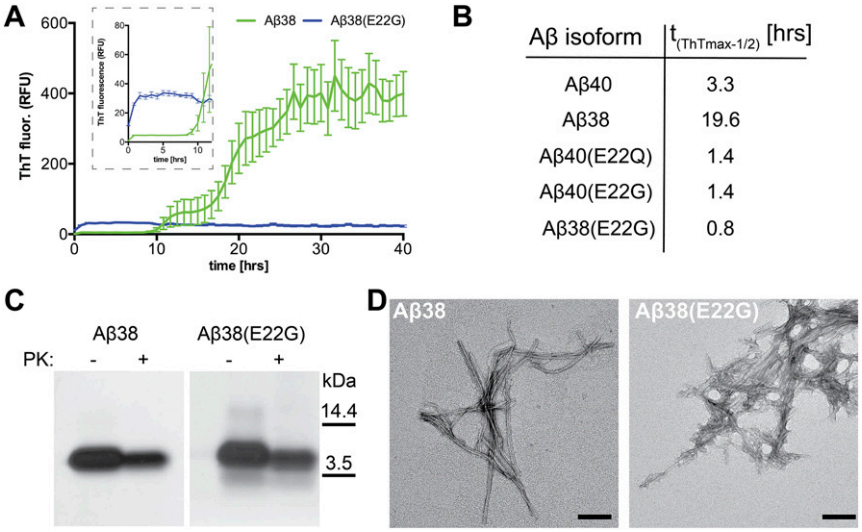

Fig. S9. Characterization of WT and mutant Aβ38 fibrils. (*A*) Fibrillization kinetics of 20 μM WT (green line) and mutant E22G (blue line) Aβ38 peptides were measured with 10 μM ThT. Synthetic WT and E22G mutant Aβ38 was incubated under constant agitation for 72 h in phosphate buffer (pH 7.2) at 37 °C. (*B*) Fibril formation propensity of all synthetic Aβ peptides used in this study is expressed as time to reach the ThT half-maximum intensity [$t_{(ThTmax-1/2)}$ (in hours)]. (*C*) Following amyloid formation, samples were centrifuged at 100,000 × *g* for 1 h, and the resulting pellet was resuspended in PBS. Synthetic Aβ38 fibrils (0.2 mg/mL in PBS) were treated with PK (0.05 mg/mL), and digestion was stopped by the addition of 1 mM PMSF after 1 h at 37 °C. PK treated (+) or untreated (–) samples were subjected to SDS/PAGE and visualized by silver staining. Amyloid formation resulted in similar amounts of PK-resistant Aβ38, independent of the E22G mutation. (*D*) Electron micrographs of Aβ38 (WT) and Aβ38 (E22G) after amyloid formation showed fibrillar aggregates with no discernable differences in ultrastructure. (Scale bars, 100 nm.)

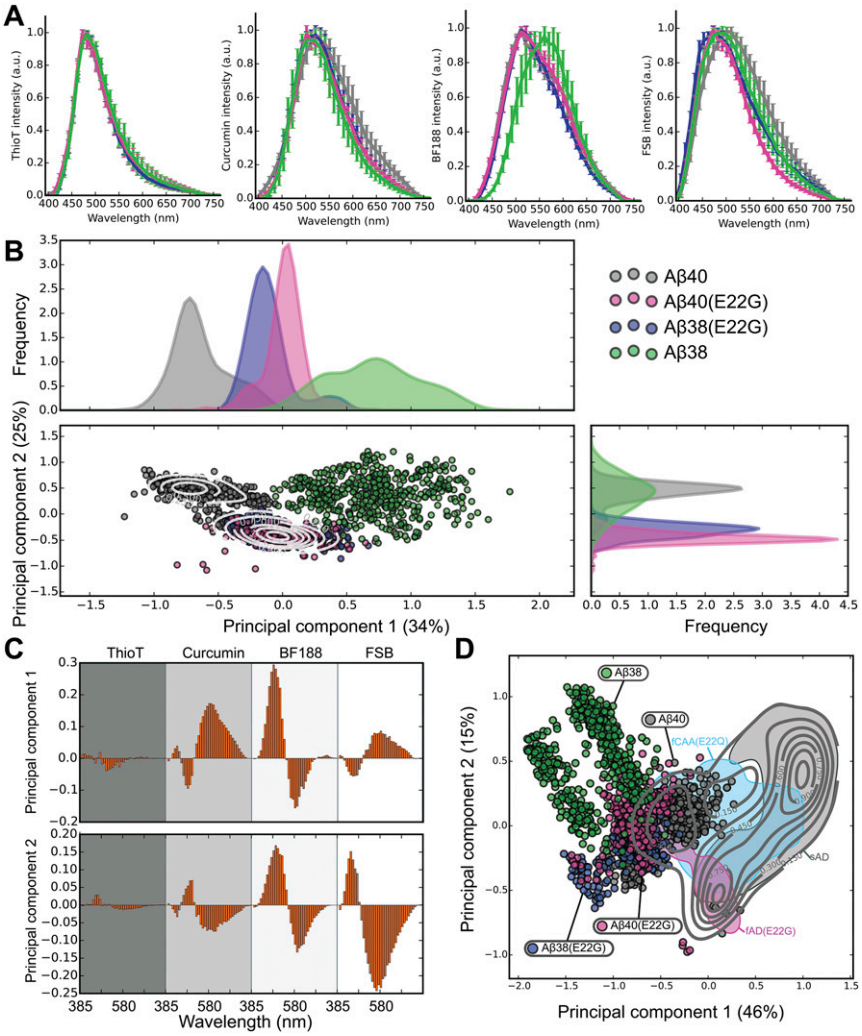

Fig. S10. Conformational variability of WT and mutant Aβ38 fibrils. (*A*) Confocal-based spectral analysis of ThT, curcumin, BF-188, and FSB fluorescence emission profiles when bound to gel-embedded Aβ38/40 fibrils with and without E22G mutations. ThT analysis: n = 3,492 aggregates. Curcumin analysis: n = 2,439 aggregates. BF-188 analysis: n = 3,748 aggregates. FSB analysis: n = 1,308 aggregates. Data shown as mean ± SD. (*B*) Projection of the multispectral vectors into the eigenspace defined by the first two principal components. (*C*) Multispectral vectors from synthetic fibrils are projected into the eigenspace defined in *B*, and their magnitudes reveal the wavelength-dependent contributions from the various dyes to the variation between the samples. (*D*) Projection of the multispectral vector into the eigenspace defined by the human and synthetic samples. The regions occupied by human sAD, fCAA [Aβ(E22Q)], and fAD [Aβ(E22G)] are shown in gray, cyan, and magenta, respectively.

Table S1. Sporadic and familial Alzheimer's disease brain samples used for analysis

Classification	ID no.	Sex	Age, y	CLDX	NPDX	Mutation	Braak Stage	APOE genotype	Brain region	Source
Sporadic AD	N1415	F	85	AD	AD		V-VI	—	Temporal cortex	Uppsala University (Sweden)
Sporadic AD	12-1181	M	62	AD	AD		VI	3/4	Frontal cortex	University of Washington (Seattle)
Sporadic AD	10-1317	F	79	AD	AD		VI	3/4	Occipital cortex	University of Washington (Seattle)
Sporadic AD	07-0997	F	87	AD	AD		VI	3/3	Occipital cortex	University of Washington (Seattle)
Sporadic AD	15-1820	M	67	AD	AD		VI	—	Frontal cortex	University of Washington (Seattle)
Sporadic AD	2217	M	63	AD	AD		VI	3/4	Middle temporal gyrus	UCSF MAC (San Francisco)
Sporadic AD	2273	M	63	AD	AD		VI	3/3	Middle temporal gyrus	UCSF MAC (San Francisco)
Sporadic AD	2312.10	M	59	AD	AD		VI	4/4	Middle temporal gyrus	UCSF MAC (San Francisco)
Sporadic AD	2371.11	M	72	AD	AD		VI	3/4	Angular gyrus	UCSF MAC (San Francisco)
Sporadic AD	2376.11	M	80	AD	AD		VI	3/3	Angular gyrus	UCSF MAC (San Francisco)
Sporadic AD	2412.12	M	88	AD	AD		VI	3/4	Angular gyrus	UCSF MAC (San Francisco)
Sporadic AD	2345.11	F	86	NCI	AD,CVD		III	3/3	Posterior ITG	UCSF MAC (San Francisco)
Sporadic AD	2509	M	103	NCI	AD		II	3/3	Posterior ITG	UCSF MAC (San Francisco)
Sporadic AD	2394.12	M	76	NCI	CAA		II	3/4	Posterior ITG	UCSF MAC (San Francisco)
Sporadic AD	BBN_6072	M	78	AD	AD,CAA, SVD		III	3/4	Frontal cortex	MRC UK Brain Bank (Manchester)
Sporadic AD	BBN_3416	M	87	AD	AD,CAA, SVD		IV	3/4	Frontal cortex	MRC UK Brain Bank (Manchester)
Sporadic AD	BBN_15592	M	62	AD	AD,LBD		—	3/4	Frontal cortex	MRC UK Brain Bank (Manchester)
Sporadic AD	BBN_2339 (SD038/14)	F	88	NCI	AD, CAA, CVD, SH		V	—	Frontal cortex	MRC UK Brain Bank (Edinburgh)
Sporadic AD	BBN_22627 (SD033/14)	F	85	NCI	AD,CAA, SH		III	—	Frontal cortex	MRC UK Brain Bank (Edinburgh)
Sporadic AD	BBN_24302 (SD040/14)	F	90	NCI	AD, CAA, SH		II	—	Frontal cortex	MRC UK Brain Bank (Edinburgh)
Sporadic AD	BBN_24306 (SD046/14)	F	83	NCI	AD, CAA, SH		III	—	Frontal cortex	MRC UK Brain Bank (Edinburgh)
fAD (Swedish)	6901	M	62	AD	AD	KM670/671NL APP	VI	3/3	Frontal cortex	Karolinska Institutet (Sweden)
fAD (Swedish)	493	M	68	AD	AD	KM670/671NL APP	—	2/3	Parietal cortex	Karolinska Institutet (Sweden)
fAD (Swedish)	39794	M	66	AD	AD	KM670/671NL APP	VI	2/3	Frontal cortex	Karolinska Institutet (Sweden)
fAD (Swedish)	7795	M	56	AD	AD	KM670/671NL APP	VI	4/4	Frontal cortex	Karolinska Institutet (Sweden)
fAD (Swedish)	14096	F	62	AD	AD	KM670/671NL APP	VI	3/3	Frontal cortex	Karolinska Institutet (Sweden)
fAD (Swedish)	0276-05	F	61	AD	AD	KM670/671NL APP	V-VI	3/4	Temporal cortex	Uppsala University (Sweden)
fAD (Arctic)	N1084	M	64	AD	AD	E693G APP (E22G Aβ)	V-VI	3/3	Temporal cortex	Uppsala University (Sweden)
fAD (Arctic)	16514	F	72	AD	AD	E693G APP (E22G Aβ)	V	—	Calcarine cortex	University of Washington (Seattle)
fAD (Arctic)	08-1041	M	67	DLB/LBD	AD,LBD	E693G APP (E22G Aβ)	VI	—	Frontal cortex	University of Washington (Seattle)
fAD (Arctic)	802	M	70	AD	AD	E693G APP (E22G Aβ)	—	3/3	Frontal cortex	Karolinska Institutet (Sweden)
fAD (Arctic)	7612	F	66	AD	AD	E693G APP (E22G Aβ)	VI	3/3	Frontal cortex	Karolinska Institutet (Sweden)
fCAA (Dutch)	E14-69-4J	F	52	CAA	CAA	E693Q APP (E22Q Aβ)	—	—	Frontal cortex	Leiden University (Netherlands)
fCAA (Dutch)	E13-99-4B	M	59	CAA	CAA	E693Q APP (E22Q Aβ)	—	—	Frontal cortex	Leiden University (Netherlands)
fCAA (Dutch)	E06-0004	M	57	CAA	CAA	E693Q APP (E22Q Aβ)	—	—	Frontal cortex	Leiden University (Netherlands)
fCAA (Dutch)	E12-82-4D	F	55	CAA	CAA	E693Q APP (E22Q Aβ)	—	—	Frontal cortex	Leiden University (Netherlands)
fCAA (Dutch)	E04-19-2B	M	51	CAA	CAA	E693Q APP (E22Q Aβ)	—	—	Frontal cortex	Leiden University (Netherlands)
fCAA (Dutch)	E05-151-2D	M	48	CAA	CAA	E693Q APP (E22Q Aβ)	—	—	Frontal cortex	Leiden University (Netherlands)
fCAA (Dutch)	E10-204-2A	F	53	CAA	CAA	E693Q APP (E22Q Aβ)	—	—	Frontal cortex	Leiden University (Netherlands)
fCAA (Dutch)	E16-84-2A	F	70	CAA	CAA	E693Q APP (E22Q Aβ)	—	—	Frontal cortex	Leiden University (Netherlands)

Colors used match those in the figure legends for sAD, fAD, fAD [Aβ(E22G)], and fCAA. Abbreviations: AD, Alzheimer's disease; APOE, Apolipoprotein E; CAA, cerebral amyloid angiopathy; CLDX, clinical diagnosis; CVD, cerebrovascular disease; DLB, dementia with Lewy bodies; F, female; M, male; MRC UK, Medical Research Council United Kingdom; NCI, no cognitive impairment; LBD, Lewy body dementia; (—): unknown; NPDX, neuropathological diagnosis; SH, sporadic hemorrhage; SVD, small vessel disease; UCSF MAC: University of California, San Francisco, Memory and Aging Center.